FEBS Letters 544 (2003) 50–56 FEBS 27265

NMR studies of the fifth transmembrane segment of sarcoplasmic reticulum Ca^{2+}-ATPase reveals a hinge close to the Ca^{2+}-ligating residues

Gerd Nielsen[a], Anders Malmendal[a], Axel Meissner[b,1], Jesper V. Møller[c], Niels Chr. Nielsen[a,*]

[a] *Interdisciplinary Nanoscience Center (iNANO) and Aarhus University NMR Center, Department of Molecular Biology, University of Aarhus, Langelandsgade 140, DK-8000 Aarhus C, Denmark*
[b] *Department of Chemistry, Carlsberg Laboratory, Gamle Carlsberg Vej 10, DK-2500 Valby, Denmark*
[c] *Department of Biophysics, University of Aarhus, DK-8000 Aarhus C, Denmark*

Received 7 March 2003; revised 15 April 2003; accepted 15 April 2003

First published online 6 May 2003

Edited by Stuart Ferguson

Abstract Two recent X-ray structures have tremendously increased the understanding of the sarco/endoplasmic reticulum Ca^{2+}-ATPase (SERCA) and related proteins. Both structures show the fifth transmembrane span (M5) as a single continuous α-helix. The inherent structural and dynamic features of this span (Lys758–Glu785) were studied in isolation in sodium dodecyl sulfate (SDS) micelles using liquid-state nuclear magnetic resonance (NMR) spectroscopy. We find that a flexible region (Ile765–Asn768) is interrupting the α-helix. The location of the flexible region near the Ca^{2+} binding residues Asn768 and Glu771 suggests that together with a similar region in M6 it has a hinge function that may be important for cooperative Ca^{2+} binding and occlusion.

Key words: Ca^{2+}-ATPase; Fifth transmembrane segment M5; Membrane protein; Micelle; Nuclear magnetic resonance; Sarcoplasmic reticulum; Sodium dodecyl sulfate

1. Introduction

Active cation transport across cell membranes as mediated by P-type ATPases like Na^+,K^+-ATPase and Ca^{2+}-ATPases is of fundamental importance for cellular processes in eukaryotic organisms, such as the formation of membrane potentials, cell volume regulation, cotransport, muscle contraction, and neurotransmission. This has motivated an enormous effort to understand the mechanistic function of these ATPases, starting with the pivotal work of Skou on Na^+,K^+-ATPase [1] and Hasselbach on sarco/endoplasmic reticulum Ca^{2+}-ATPase (SERCA) [2] in the fifties and sixties. These have been followed by a large body of kinetic, mutagenesis, and topological studies [3–8] and more detailed structural studies by electron microscopy [9–11], X-ray diffraction (XRD) [12–14], and nuclear magnetic resonance (NMR) spectroscopy [15–17].

Among the many P-type ATPases, the SERCA is the most well-characterized system at the structural and functional level. SERCA has a molecular weight of 110 kDa distributed on three large cytoplasmic domains and a membrane-bound domain, comprising 10 transmembrane helices as illustrated in Fig. 1 using the XRD coordinates for Ca^{2+}-free SERCA determined by Toyoshima et al. [14]. This 3.1 Å resolution XRD structure, and an earlier 2.6 Å XRD structure for SERCA in Ca^{2+}-bound form [13], form a unique basis for more detailed functional analysis of mechanisms involved in the reaction cycle. In short, the reaction cycle can be described by four steps: $E_1 \rightarrow E_1P \rightarrow E_2P \rightarrow E_2 \rightarrow E_1$, where E_1 and E_2 are the two major conformational states and P indicates states phosphorylated by adenosine triphosphate (ATP). During the $E_1P \rightarrow E_2P$ transition, Ca^{2+} is released from the high-affinity E_1 states on the lumenal side of the membrane. However, structural [12–14] and modelling [14,18] studies as well as deductions made from the primary sequence [19], mutagenesis [3,4,20,21] and biophysical experiments [22,23] reveal a large separation between the ATP binding and phosphorylation sites in the cytoplasmic domain and the Ca^{2+} binding sites in the transmembrane domain. This has led to speculations as to how conformational changes are transmitted between the intra-membranous and cytosolic domains to enable the ATPases (i) to become phosphorylated by ATP after cation binding, and subsequent to phosphorylation (ii) to transport cations through the membrane. Such changes will, in addition to the proposed extensive movements of the cytosolic domains in Ca^{2+}-ATPase [12,14] and Na^+,K^+-ATPase [24,25], require substantial flexibility of the highly conserved M4, M5, M6, and M8 helices [4] which all contain residues involved in cation binding.

With respect to these issues, it should be borne in mind that the XRD structures provide static snapshots of the E_1 and E_2 states, that the E_2 state is stabilized by the potent inhibitor thapsigargin and therefore not identical to the inhibitor-free E_2 state, and that the resolution (2.6 and 3.1 Å, respectively) is not sufficiently high to fully characterize the details of local structure. Focusing on the Ca^{2+} binding sites, it remains interesting to study the structural flexibility in proximity of critical residues such as Asn768, Gly770, and Glu771 in the fifth transmembrane segment M5, a segment extensively studied by site-directed mutagenesis [3,5,26–30]. It is not unlikely that structures with a flexible segment in the middle of the membrane helix would be better suited for the structural rearrangements required for Ca^{2+} binding and translocation than the seemingly stiff α-helical structures revealed by XRD. To examine these aspects, we have in this paper undertaken a high-resolution NMR structural analysis of the isolated Lys758–Glu785 (M5) membrane span in sodium dodecyl sul-

*Corresponding author. Fax: (45)-86-196199.
E-mail address: ncn@imsb.au.dk (N.C. Nielsen).

[1] Present address: Novartis Pharma AG, CH-4002 Basel, Switzerland.

0014-5793/03/$22.00
doi:10.1016/S0014-5793(03)00448-4

fate (SDS) micelles. This study was motivated by the fact that NMR is a very sensitive probe for local structure and flexibility, although it is clear that the M5 segment is not in its native environment and thus lacks the interactions with the surrounding transmembrane helices. The usefulness of this approach, however, is supported by the fact that previous structural analysis of membrane segments of membrane proteins such as bacteriorhodopsin [31–33], rhodopsin [34,35], F_1-F_0-ATPase [36], and also previously the M6 segment of SERCA [15] in hydrophobic media proves to be in good agreement with existing structures on membrane proteins [14,18,37–39].

2. Materials and methods

2.1. Sample preparation

The 28-residue M5 peptide, acetyl-KQFIR YLISS NVGEV VSIFL TAALG LPE-amide corresponding to Lys758–Glu785 of the fifth membrane span of SERCA, was purchased from SynPep Corporation (Dublin, CA, USA). The peptide was synthesized using Fmoc chemistry, with the N-terminal acetylated and the C-terminus blocked by an amino group. The sequence was verified by mass spectrometry and the purity was determined to be 95.5% by high-performance liquid chromatography (HPLC). The M5 peptide was reconstituted into fully deuterated SDS micelles by adding M5 peptide to a solution containing 400 mM SDS-d_{25} (Cambridge Isotope Laboratories, Andover, MA, USA), 100 mM NaCl, 20 mM sodium phosphate (pH 7.0), 1 mM NaN_3, and 10% D_2O (90% H_2O). The final peptide concentration was 2.4 mM.

2.2. NMR spectroscopy

All NMR spectra were recorded on a Bruker 600 MHz NMR spectrometer operating at a ^1H frequency of 600.13 MHz (14.1 T). Phase-sensitive (States-TPPI [40]) ^1H double-quantum filtered correlated spectroscopy (DQF-COSY) [41,42], total correlation spectroscopy (TOCSY) [43,44] (40 and 65 ms DIPSI-2 mixing [45]), and nuclear Overhauser effect spectroscopy (NOESY) [46,47] (100 and 170 ms mixing) experiments were recorded at 313 K. The water signal was suppressed using weak presaturation (2 s). All spectra were recorded with a spectral width of 6361 Hz in both dimensions. Data matrices of 840×1024 points for the DQF-COSY spectra and 640×1024 points for the TOCSY and NOESY spectra, respectively, were zero filled to 1024×2048 points prior to Fourier transformation. The DQF-COSY spectra were apodized using a sine window function shifted by $\pi/4$ in the t_1 and $\pi/6$ in the t_2 dimension, respectively, while for the TOCSY and NOESY spectra a cosine window function was applied in both dimensions. All spectra were processed using the Bruker XWINNMR software and analyzed using PRONTO [48].

2.3. Structure calculations

The secondary structure of the peptide was analyzed qualitatively using $^3J_{HNH\alpha}$ coupling constants extracted from the DQF-COSY spectra, and $^1H^\alpha$ chemical shift indices (CSI) [49,50]. Distance constraints were obtained from the 170 ms NOESY spectra using the integration tool in PRONTO and categorized as strong (<3.0 Å), medium (<3.5 Å), and weak (<6.0 Å). The spectra revealed 284 intra-residue, 127 sequential, and 153 medium range NOEs. The structures were calculated using the crystallography & NMR system (CNS) [51], starting with extended structures [52], and using the torsion angle dynamics (TAD) procedure [53] with NOE scale factors of 200, 200, 200, and 100 and temperature steps of 50 and 10 K in the first and second slow-cooling periods, respectively. 50 structures were generated of which the 40 with lowest energy were selected for analysis. These structures had no NOE violations >0.2 Å, and analysis by PROCHECK [54,55] showed that backbone torsion angles for 78.9%, 19.7%, 0.8%, and 0.7% of the residues are in the 'most favored', 'additional allowed', 'generously allowed', and 'disallowed' regions respectively. Root-mean-square deviation (RMSD) calculations and superposition were performed using MOLMOL [56]. The secondary structure of the peptide was also predicted from the amino acid sequence using the Rost and Sander procedure available on the Protein Predict Server [57].

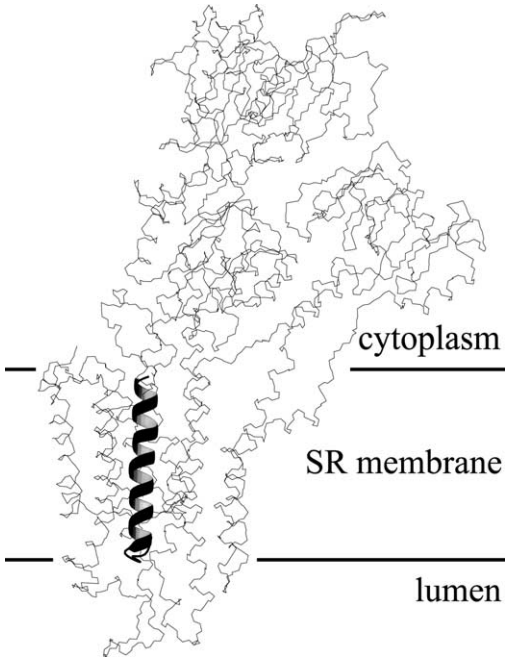

Fig. 1. The XRD structure of Ca^{2+}-free SERCA (Protein Data Bank, PDB, code 1IWO) [14] with the 28-residue M5 peptide represented in ribbon form.

3. Results

Combination of data from the DQF-COSY, TOCSY, and NOESY experiments allowed assignment of all ^1H resonances using the procedures of Wüthrich [58]. To illustrate the quality of the spectra, Fig. 2 shows selected regions of the two-dimensional (2D) NOESY spectrum. The many strong H^N–H^N correlations indicate a helical conformation in at least part of the peptide. This interpretation is further supported by the full NOE connectivity pattern, the distribution of intra- and inter-residue NOEs, $^3J_{HNH\alpha}$ coupling constants, and H^α CSI, as summarized in Fig. 3A–C. The NOE pattern (Fig. 3A) and distribution (Fig. 3D) indicate two α-helical regions extending over Lys758–Leu764 and Val769–Ala779 through the presence of a large number of $d_{\alpha N}(i,i+3)$ and $d_{\alpha\beta}(i,i+3)$ correlations in these regions. The $^3J_{HNH\alpha}$ coupling constants are indicative of α-helical structures in the Lys758–Ile765 and Val769–Leu781 regions (Fig. 3B). The CSI method, where the $^1H^\alpha$ chemical shifts are compared with random coil values, suggests slightly shorter α-helices extending over Ile761–Leu764 and Glu771–Thr778 (Fig. 3C). The sequence analysis from the Protein Predict Server [57] generally agrees with the NMR data, with α-helices being predicted for Gln759–Ser766 and Val769–Ala780 (Fig. 3E).

Confronted with the fact that two protons only need to be in close contact part of the time to give a significant NOE cross-peak, it is relevant to estimate the helical content on basis of the $^3J_{HNH\alpha}$ coupling constants as described by Bradley et al. [59]. The measured coupling constants $^3J_{HNH\alpha}$ are compared with a typical random coil coupling constant, $^3J_{rc}=8$ Hz, and α-helical coupling constant, $^3J_{helix}=4$ Hz, to calculate the overall helical content as $(^3J_{HNH\alpha}-{}^3J_{rc})/(^3J_{helix}-{}^3J_{rc})$. For Lys758–Ile765 and Val769–Leu781 a conservative estimate is a helical population above 50%.

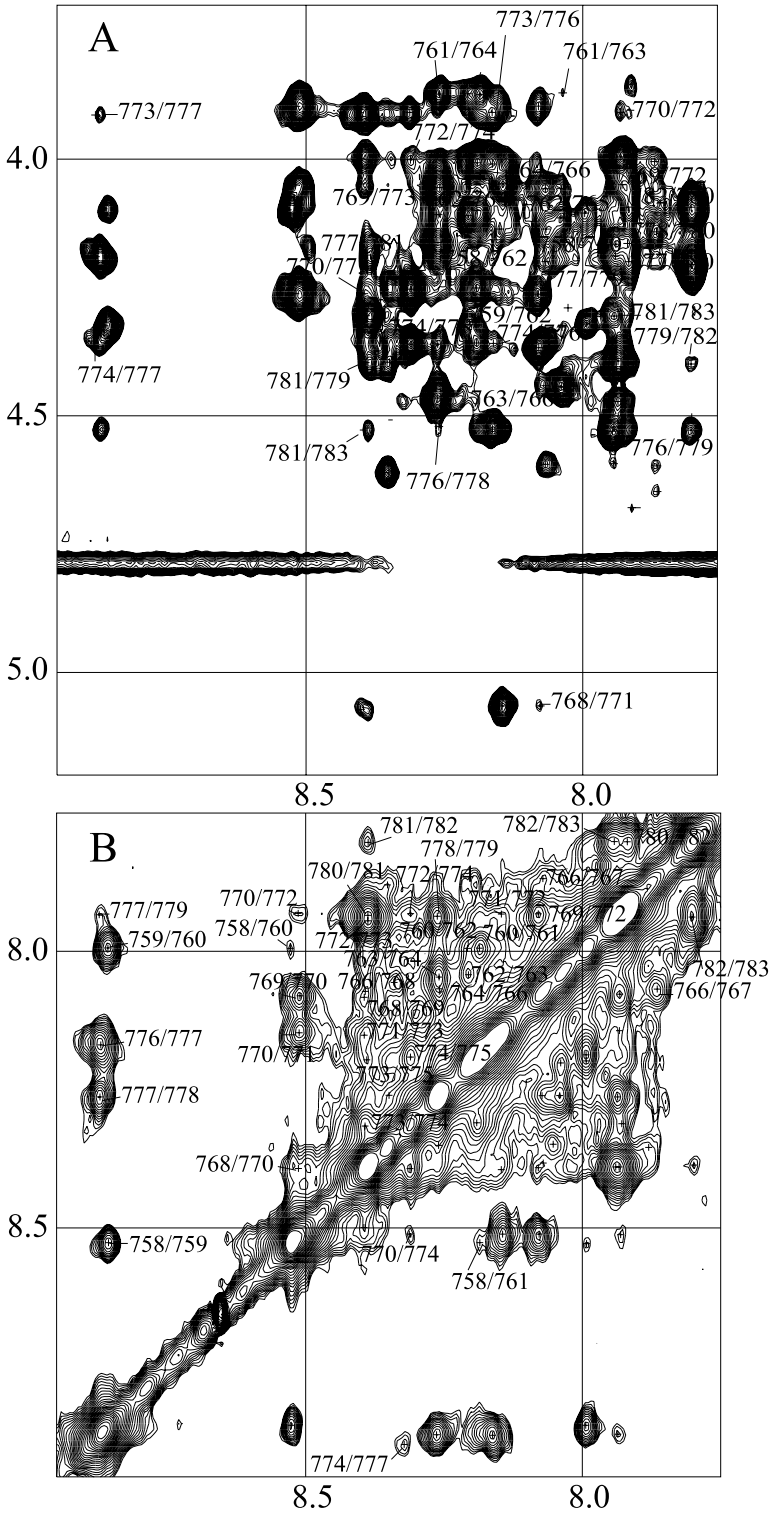

Fig. 2. Selected regions of the 170 ms 2D NOESY spectrum of the M5 peptide in SDS micelles. A: Fingerprint H^{α}–H^{N} region. B: Amide H^{N}–H^{N} region. For clarity, only NOEs between non-neighboring residues are shown in A.

Since an uninterrupted and rather rigid α-helical structure is expected from the XRD structures of Toyoshima and coworkers [13,14], it is relevant to address specific attention to the intermediate flexible region. This region shows typical random coil $^{3}J_{HNH\alpha}$ couplings and chemical shifts, and lacks the medium range NOEs typical of ordered structure, as is clearly shown when overlaying the 40 lowest energy structures (Fig. 4). The structures are all largely α-helical, but the relative orientation of the two helical segments varies from structure to structure. As illustrated in Fig. 3F, superposition of the full peptide results in an averaged backbone RMSD of 2.8 Å, which compares unfavorably with typical values of

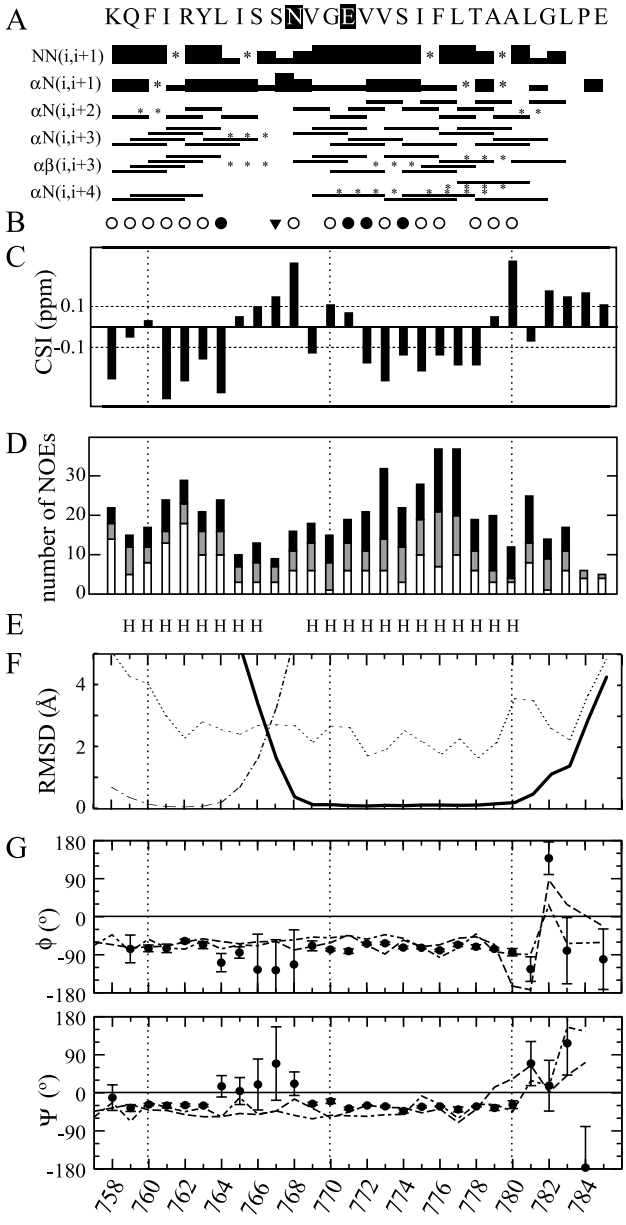

Fig. 3. Summary of structural parameters for M5 in SDS micelles. The peptide sequence with the putative Ca^{2+} binding sites indicated with black squares is shown in the top. A: Sequential and medium range NOEs with thicker lines indicating higher NOE intensity, and asterisks indicating NOEs that can not be unambiguously identified due to overlap with other signals. B: $^3J_{HNH\alpha}$ coupling constants with filled circles, open circles, and filled triangles (non-glycine residues) representing coupling constants less than 5 Hz, less than 6 Hz, and above 8 Hz, respectively. C: $^1H^{\alpha}$ CSI using random coil values from [50]. D: NOE distribution with white, shaded, and black bars representing intra-residual, sequential, and medium range NOEs, respectively. E: Helix propensities (indicated by H) obtained using the Protein Predict Server [57]. F: RMSD values for MOLMOL alignment of the 40 best structures in the regions Phe760–Leu764 (dot-dashed line), Val769–Ala780 (solid line), and the full peptide (dashed line). G: ϕ and ψ backbone torsion angles with the bars showing the distribution (standard deviations) over the 40 analyzed NMR structures (black circles), and the ϕ and ψ backbone torsion angles for the XRD structures of the Ca^{2+}-bound E_1 form (PDB code: 1EUL; dashed line) [13] and the Ca^{2+}-free E_2 form (PDB code: 1IWQ; dot-dashed line) [14].

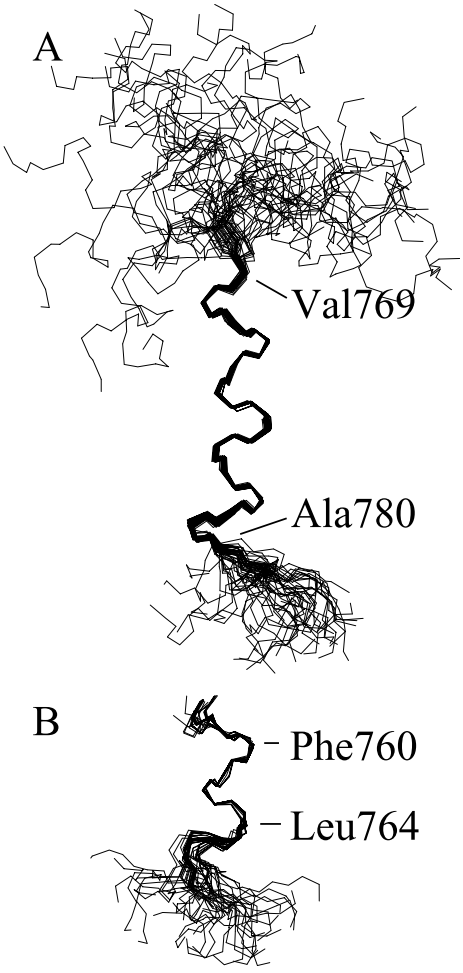

Fig. 4. Superposition of the 40 lowest-energy structures calculated for the M5 transmembrane peptide using (A) residues Val769 to Ala780 and (B) Phe760 to Leu764. Residues Lys758 to Glu785 (A) and Lys758 to Asn768 (B) are shown.

0.3–0.6 Å for α-helices in globular proteins. Superposition of the peptides confined to either of the established helical regions, Phe760–Leu764 and Val769–Ala780, leads to the much lower backbone RMSD values of 0.15 Å and 0.16 Å, respectively. The localization of structure and disorder is also illustrated by the backbone torsion angles of the 40 lowest energy structures as shown in Fig. 3G. Disordered regions are also found in the N- and C-termini (Lys758–Gln759 and Leu781–Glu785, respectively), starting near the limits of the expected membrane spanning segment. However, although the last five C-terminal residues show significant disorder, NMR structure backbone torsion angles follow a pattern that is similar to what is seen in the XRD structures, indicating that the structural feature of the full protein is retained also near an artificial ending in an aqueous environment.

4. Discussion

The finding that the transmembrane part of the SERCA M5 helix contains a flexible hinge region near Asn768 and Glu771 in membrane-like environments is interesting for several reasons. It offers new perspectives on the structural information from the recent XRD studies [13,14], which show

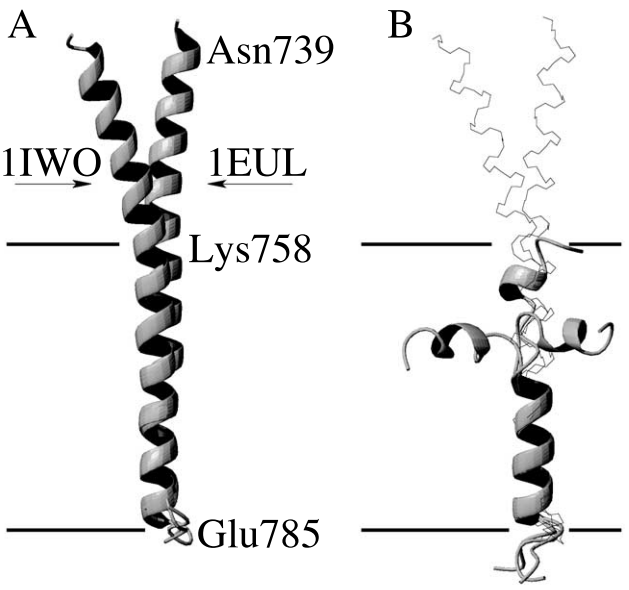

Fig. 5. Ribbon representation of (A) the full M5 helix (Asn739–Glu785) determined by Toyoshima et al. for the Ca^{2+}-bound E_1 form (PDB code: 1EUL) [13] and the Ca^{2+}-free E_2 form (PDB code: 1IWQ) [14] and (B) superposition of the three best NMR structures in a ribbon representation aligned with the XRD structures in a line representation. All structures were aligned using the Val769–Ala780 region.

one straight α-helix, and adds structural evidence related to earlier mutagenesis- and modelling-based models on Ca^{2+} binding/release in SERCA [3,5–7,20,26–29,60]. Along with Thr799 and Asp800 (in M6) and Glu908 (in M8), Asp768 and Glu771 are considered strong candidates as donors of oxygen ligands for Ca^{2+} binding in the first binding site (I), while Glu309 in M4 and Asn796 and Asp800 in M6 together with the carbonyl oxygens of Val304, Ala305, and Ile307 in M4 act as donors to Ca^{2+} binding at site II [13,14]. A crucial role of Glu771, together with Thr799 and Asp800 is emphasized by mutation experiments which indicate that these residues are necessary not only for Ca^{2+} binding at site I, but also for cooperative interaction between the two Ca^{2+} sites [6,7,27,29,60]. It has been suggested that in the Ca^{2+}-free E_2 form the Ser767 and Asn768 sidechains may be involved in hydrogen bonding to the carboxyl groups in the Ca^{2+}-ligating Glu771 and Asp800 residues [14]. In addition, site-directed mutagenesis has revealed that Gly770 together with Gly310 and Gly801, all of which are located next to the glutamic and aspartic Ca^{2+} ligands in M4, M5, and M6, are important for Ca^{2+} binding and dissociation [27]. Substitution of these glycines by amino acids with bulky sidechains [27] had a dramatic negative effect on the Ca^{2+} affinity, which indicates either that flexibility in proximity of the carboxylic residues is required for the Ca^{2+} binding and occlusion mechanism, or that the Ca^{2+} transport is sterically hindered by a bulkier sidechain. In this context it is of interest to note that, as first noted by Rice and MacLennan [29], the putative calcium binding M4, M5, and M6 helices all share the same sequence motif Asp/Glu Gly Leu/Val (reversed in M5), located approximately in the center of the membrane spanning segment, and that the helices are interrupted in M4 and M6 [13,15]. Finally, addressing the shorter N-terminal helix Phe760–Leu764, there is evidence that substitution of Tyr763 by Gly uncouples the Ca^{2+} transport from the Ca^{2+}-activated ATP hydrolysis [61]. This could indicate that a rotation of this helix with the bulky tyrosine sidechain, relative to the C-terminal part of the M5 segment, is involved in the gating of Ca^{2+} influx from the cytosolic side as suggested previously [3].

Taken together, most of the previous models appear compatible with the present NMR structure, which shows flexibility in the central Leu764–Asn768 region. This flexibility may account for movements required to establish the necessary coordination for Ca^{2+} binding and occlusion as well as the hydrogen bonding interactions needed to stabilize the structure in the different states. While the XRD structures of SERCA [13,14] appear to be compatible with the flexible hinge in M6 found in an earlier liquid-state NMR study of this segment in micelles [15], they have not revealed a similar flexibility for the transmembrane part of M5. Instead this segment is presented as a largely straight α-helix in the E_1 state [13], and an α-helix which is slightly curved in the cytosolic extension of M5 into S5 in the E_2 state [14]. However, an increase in the B factors for Ile765–Glu771 for the Ca^{2+}-free E_2 state [14] could suggest some mobility in this region. For illustration Fig. 5A shows the entire backbone of the M5/S5 helix from both XRD structures in a ribbon mode. The larger structural flexibility offered by the NMR structure is illustrated in Fig. 5B, where the three lowest energy structures are compared to the XRD structures. While this flexibility may appear surprising relative to the XRD structure, it should be noted that secondary structure prediction calculations are in support of the presence of hinge regions in the membrane center of M5 as well as in the N-terminal cytoplasmic boundary region. Clearly, there is very good agreement between the XRD and NMR structures in the C-terminal Gly770–Ala780 part of M5, which in both cases is described as an amphiphatic helix with a hydrophilic/charge lining composed of Glu770, Ser774, and Thr778 on one side of an overall hydrophobic surface. It should be noted that the large variation in the bend angle of the hinge shown for the NMR structures is likely to be a consequence of lack of structurally ordered protein context and incorporation in a micellar non-ordered environment, and that the degree of flexibility in this region may be altered within the context of the full molecule.

It is interesting to note that the flexible region Leu764–Asn768 of M5, as revealed here, has a very similar location in the membrane compared to the flexible region Thr799–Asp800 in M6, in support of the presence of a flexible Ca^{2+} binding cavity between the helices M4, M5, and M6 [15]. Flexibility may also have consequences for the details of the conformational changes occurring during the Ca^{2+}-ATPase cycle. Thus, it has been proposed that rotation of the stiff M5 membrane span around a pivotal point close to Gly770 is important for coupling motions in the membrane Ca^{2+} binding site and the cytoplasmic phosphorylation site associated with the E_1 to E_2 transition [14]. Indeed, the evidence of flexibility for certain regions of the M5/S5 helix provided by our study can be seen as support for the bending of the chain which has been described especially in the E_2 state [14]. Here we note that the degree of flexibility is likely to depend on the presence of bound Ca^{2+} and the actual state in the cycle. The ordered helical structure for this segment described in the E_1 structure [13], together with an increase in the B factors of the hinge in the E_2 structure [14], suggests that this indeed is the

case. A relatively stiff state of the M5/S5 helix in the E_1 state may also provide a structural basis for the linkage between Ca^{2+} binding and phosphorylation by ATP present under these conditions, e.g. by charge transduction through a series of hydrogen bonds in continuous α-helices as has been recently proposed [30]. Deeper insight into the detailed structure and dynamics of active Ca^{2+} transport by SERCA may be obtained in studies of larger fragments of the membrane domain, using liquid-state NMR techniques and solid-state NMR on oriented samples [62,63], giving details on structure and dynamics, of e.g. a significant part of a Ca^{2+} site, in a micelle system, as well as the conformation and orientation in a phospholipid bilayer membrane.

5. Supporting material

^{1}H chemical shifts for M5 in SDS micelles have been deposited in the BioMagResBank (BMRB accession code 5765).

Acknowledgements: We acknowledge Dr. Marc le Maire for stimulating and fruitful discussions and for valuable comments on the manuscript, and the Carlsberg Laboratory for the use of the Bruker 600 MHz spectrometer. This research was funded by grants from Novo Nordisk Fonden, Carlsbergfondet, The Danish Biotechnological Instrument Centre (DABIC), The Danish Natural Science Council, and The University of Aarhus Research Foundation.

References

[1] Skou, J.C. (1957) Biochim. Biophys. Acta 23, 394–401.
[2] Hasselbach, W. (1964) Prog. Biophys. Biophys. Chem. 14, 169–222.
[3] Andersen, J.P. (1995) Biosci. Rep. 15, 243–261.
[4] Møller, J.V., Juul, B. and le Maire, M. (1996) Biochim. Biophys. Acta 1286, 1–51.
[5] Chen, L., Sumbilla, C., Lewis, D., Zhong, L., Strock, C., Kirtley, M.E. and Inesi, G. (1996) J. Biol. Chem. 271, 10745–10752.
[6] Strock, C., Cavagna, M., Peiffer, W.E., Sumbilla, C., Lewis, D. and Inesi, G. (1998) J. Biol. Chem. 273, 15104–15109.
[7] Inesi, G., Zhang, Z. and Lewis, D. (2002) Biophys. J. 83, 2327–2332.
[8] MacLennan, D.H., Rice, W.J. and Green, N.M. (1997) J. Biol. Chem. 272, 28815–28818.
[9] Toyoshima, C., Sasabe, H. and Stokes, D.L. (1993) Nature 362, 467–471.
[10] Auer, M., Scarborough, G.A. and Kühlbrandt, W. (1998) Nature 392, 840–843.
[11] Hebert, H., Hurhonen, P., Vorum, H., Thomsen, K. and Maunsbach, A. (2001) J. Mol. Biol. 314, 479–494.
[12] Zhang, P., Toyoshima, C., Yonekura, K., Green, N.M. and Stokes, D.L. (1998) Nature 392, 835–839.
[13] Toyoshima, C., Nakasako, M., Nomura, H. and Ogawa, H. (2000) Nature 405, 647–655.
[14] Toyoshima, C. and Nomura, H. (2002) Nature 418, 605–611.
[15] Soulié, S., Neuman, J.-S., Berthomieu, C., Møller, J.V., le Maire, M. and Forge, V. (1999) Biochemistry 38, 5813–5821.
[16] Menguy, T., Corre, F., Juul, B., Bouneau, L., Lafitte, D., Derrick, P.J., Sharma, P.S., Falson, P., Levine, B.A., Møller, J.V. and le Maire, M. (2002) J. Biol. Chem. 277, 13016–13028.
[17] Abu-Abed, M., Mal, T.K., Kainosho, M., MacLennan, D.H. and Ikura, M. (2002) Biochemistry 41, 1156–1164.
[18] Xu, C., Rice, W.J., He, W. and Stokes, D.L. (2002) J. Mol. Biol. 316, 201–211.
[19] Brandl, C.J., Green, N.M., Korczak, B. and MacLennan, D.H. (1986) Cell 44, 597–607.
[20] Clarke, D.M., Loo, T.W., Inesi, G. and MacLennan, D.H. (1989) Nature 339, 476–478.
[21] Clarke, D.M., Loo, T.W. and MacLennan, D.H. (1990) J. Biol. Chem. 265, 22223–22227.
[22] Bigelow, D.J. and Inesi, G. (1992) Biochim. Biophys. Acta 1113, 323–338.
[23] Baker, K.J., East, J.M. and Lee, A.G. (1994) Biochim. Biophys. Acta 1147, 6–12.
[24] Patchornik, G., Goldshleger, R. and Karlish, S.J.D. (2000) Proc. Natl. Acad. Sci. USA 97, 11954–11959.
[25] Patchornik, G., Munson, K., Goldshleger, R., Shainskaya, A., Sachs, G. and Karlish, S.J.D. (2002) Biochemistry 39, 11740–11749.
[26] Andersen, J.P., Vilsen, B. and MacLennan, D.H. (1992) J. Biol. Chem. 267, 2767–2774.
[27] Andersen, J.P. and Vilsen, B. (1992) J. Biol. Chem. 267, 19383–19387.
[28] Andersen, J.P. and Vilsen, B. (1998) Trends Cardiovasc. Med. 8, 41–48.
[29] Rice, W.J. and MacLennan, D.H. (1996) J. Biol. Chem. 271, 31412–31419.
[30] Scarborough, G.A. (2002) J. Bioenerg. Biomembr. 34, 235–250.
[31] Barsukov, I.L., Abdulaeva, G.V., Arseniev, A.S. and Bystrov, V.F. (1990) Eur. J. Biochem. 192, 321–327.
[32] Lomize, A.L., Pervushin, K.V. and Arseniev, A.S. (1992) J. Biomol. NMR 2, 361–372.
[33] Pervushin, K.V. and Arseniev, K.V. (1992) FEBS Lett. 308, 190–196.
[34] Chopra, A., Yeagle, P.L., Alderfer, J.A. and Albert, A.D. (2000) Biochim. Biophys. Acta 1463, 1–5.
[35] Yeagle, P.L., Danis, C., Choi, G., Alderfer, J.L. and Albert, A.D. (2000) Mol. Vis. 6, 125–131.
[36] Girvin, M.E., Rastogi, V.K., Abildgaard, F., Markley, J.L. and Fillingame, R.H. (1998) Biochemistry 37, 8817.
[37] Luecke, H., Schobert, B., Richter, H.-T., Cartailler, J.-P. and Lanyi, J.K. (1999) J. Mol. Biol. 29, 899–911.
[38] Palczewski, K., Kumasaka, T., Hori, T., Behnke, C.A., Motoshima, H., Fox, B.A., Le Tronog, I., Teller, D.C., Okada, T., Stenkamp, R.E., Yamamoto, M. and Miyano, M. (2000) Science 289, 739–745.
[39] Stock, D., Leslie, A.G. and Walker, J.E. (1999) Science 286, 1700–1705.
[40] Marion, D., Ikura, M., Tschudin, R. and Bax, A. (1989) J. Magn. Reson. 85, 393–399.
[41] Rance, M., Sørensen, O.W., Bodenhausen, G., Wagner, G., Ernst, R.R. and Wüthrich, K. (1983) Biochem. Biophys. Res. Commun. 117, 479–485.
[42] Derome, A. and Williamson, M. (1990) J. Magn. Reson. 88, 177–185.
[43] Braunschweiler, L. and Ernst, R.R. (1983) J. Magn. Reson. 53, 521–528.
[44] Bax, A. and Davis, D.G. (1985) J. Magn. Reson. 65, 355–360.
[45] Jeener, J., Meier, B.H., Bachmann, P. and Ernst, R.R. (1979) J. Chem. Phys. 71, 4546–4553.
[46] Macura, S., Huang, Y., Suter, D. and Ernst, R.R. (1981) J. Magn. Reson. 43, 259–281.
[47] Shaka, A.J., Lee, C.J. and Pines, A. (1988) J. Magn. Reson. 77, 274–293.
[48] Kjær, M., Andersen, K.V. and Poulsen, F.M. (1994) Methods Enzymol. 239, 288–307.
[49] Wishart, D.S., Richards, F.M. and Sykes, B.D. (1992) Biochemistry 31, 1647–1651.
[50] Wishart, D.S. and Sykes, B.D. (1994) Methods Enzymol. 239, 363–392.
[51] Brünger, A.T., Adams, P.D., Clore, M., deLano, W.L., Gros, P., Gross-Kunstleve, R.W., Jiang, J.-S., Kuszewski, J., Nilges, M., Pannu, N.S., Read, R.J., Rice, L.M., Simonson, T. and Warren, G.L. (1998) Acta Cryst. D54, 905–921.
[52] Nilges, M., Gronenborn, A.M., Brünger, A.T. and Clore, G.M. (1988) Protein Eng. 2, 27–38.
[53] Stein, E.G., Rice, L.M. and Brünger, A.T. (1997) J. Magn. Reson. 124, 154–164.
[54] Laskowski, R.A., MacArthur, M.W., Moss, D.S. and Thornton, J.M. (1993) J. Appl. Cryst. 26, 283–291.
[55] Morris, A.L., MacArthur, M.W., Hutchinson, E.G. and Thornton, J.M. (1992) Proteins 12, 345–364.
[56] Koradi, R., Billeter, M. and Wüthrich, K. (1996) J. Mol. Graph. Model. 14, 51–55.

[57] Rost, B. and Sander, C. (1993) J. Mol. Biol. 232, 584–599.
[58] Wüthrich, K. (1986) NMR of Proteins and Nucleic Acids, Wiley, New York.
[59] Bradley, E.K., Thomason, J.F., Cohen, F.E., Rosen, P.A. and Kuntz, I.D. (1990) J. Mol. Biol. 215, 607–622.
[60] Zhang, Z., Lewis, D., Strock, C., Inesi, G., Nakasako, M., Nomura, H. and Toyoshima, C. (2000) Biochemistry 39, 8758–8767.
[61] Andersen, J.P. (1995) J. Biol. Chem. 270, 908–914.
[62] Opella, S.J. (1997) Nat. Struct. Biol. 4, 845–848.
[63] Vosegaard, T. and Nielsen, N.C. (2002) J. Biomol. NMR 22, 225–247.